

A kinetic study on *para*-fluoro-thiol reaction in view of its use in materials design

*Federica Cavalli,^a Lies De Keer,^b Birgit Huber,^a Paul H. M. Van Steenberge,^c Dagmar R. D'hooge,^{*b,c} Leonie Barner^{*a,d}*

- a. Soft Matter Synthesis Laboratory, Institut für Biologische Grenzflächen, Karlsruhe Institute of Technology (KIT), Hermann-von-Helmholtz-Platz 1, 76344, Eggenstein-Leopoldshafen, Germany.
- b. Laboratory for Chemical Technology (LCT), Ghent University, Technologiepark 125, 9052 Zwijnaarde (Ghent), Belgium; E-Mail: dagmar.dhooge@ugent.be
- c. Centre for Textile Science and Engineering (CTSE), Ghent University, Technologiepark 70A, 9052 Zwijnaarde (Ghent), Belgium
- d. School of Chemistry, Physics and Mechanical Engineering and Institute of the Future Environments, Queensland University of Technology (QUT), 2 George Street, QLD 4000, Brisbane, Australia. E-Mail: leonie.barner@qut.edu.au

Contents:

1. Full characterization for PS1 and PS2 obtained via RAFT polymerization

- 1.1. Table S1 - Overview of the reactions and rate coefficients for PS1 and PS2 during RAFT polymerizationS4
- 1.2. Section S1a – apparent termination rate coefficient.....S5
 - 1.2.1. Table S2 - Parameters used for the composite k_t model4.....S5
- 1.3. Section S1b - Apparent conventional initiator efficiency.....S6
 - 1.3.1. Table S3 – Description and value of the parameters used.....S6
- 1.4. Figure S1 – Experimental and simulated (kMC) RAFT polymerization kinetic for PS1 (left) and (right) PS2.....S7
- 1.5. Figure S2 to S4, $^1\text{H-NMR}$ and $^{13}\text{C-NMR}$ (S2), SEC traces (S3), and ESI-MS spectra (S4) for PS1 and PS1-SH. In Figure S3 the GPC traces for PS1b and PS1b-SH are also reported.....S8
- 1.6. Figure S5 to S7, $^1\text{H-NMR}$ and $^{13}\text{C-NMR}$ (S5), SEC traces (S6), and ESI-MS spectra (S7) for PS2 and PS2-SH.....S11

2. Characterization for 1PFB

- 2.1. Figure S8 - $^1\text{H-NMR}$ spectrum (400 MHz, CDCl_3) of 1PFBS14
- 2.2. Figure S9 - $^{13}\text{C-NMR}$ spectrum (100 MHz, CDCl_3) of 1PFB.....S14
- 2.3. Figure S10 - $^{19}\text{F-NMR}$ spectrum (CDCl_3 , 376 MHz) of 1PFB.....S15

3. Determination of the PFB conversion via $^{19}\text{F-NMR}$

- 3.1. Figure S11 - Representative $^{19}\text{F-NMR}$ spectrum (CDCl_3 , 376MHz) of a selected sample from the kinetic study. Calculation of the conversion via $^{19}\text{F-NMR}$S16

4. Summary of all the reaction conditions explored in the study

- 4.1. Table S4 – Sum up of all the reaction conditions for disulfide bond formation.....S17
- 4.2. Table S5 – Sum up of all the reaction conditions for PFTRS18

5. Kinetic modelling (reactions performed without TCEP)

- 5.1. Section S5a – SEC broadening.....S19
 - 5.1.1. For low molar mass thiol derivatives.....S19
 - 5.1.2. For polymeric thiols.....S19
 - 5.1.2.1. Figure S12 – SEC broadening for polystyrene (PS) standard.....S20
- 5.2. Investigation on PFTR and disulfide bond formation reaction for low molar mass thiol derivatives
 - 5.2.1. Figure S13 – Experimental and simulated main and side reaction for low molar mass thiol derivatives.....S21
 - 5.2.2. Figure S14 – Simulated product spectrum for thiol **3**.....S23
 - 5.2.3. Figure S15 Comparison of PFTR kinetic for thiols **1** to **5**.....S24
- 5.3. Investigation on PFTR and disulfide bond formation reaction for polymeric thiols
 - 5.3.1. Figure S16 – Equilibrium reaction for disulfide bond formation in DMF.....S25
 - 5.3.2. Figure S17 – Full PFTR kinetic for PS1-SH and PS2-SH.....S26
 - 5.3.3. Figure S18 – SEC traces for the evolution of PFTR for PS1-SH in THF and DMF.....S27
 - 5.3.4. Figure S19 – Influence of shielding due to the substitution degreeS28
 - 5.3.5. Figure S20 - Evolution of the mono-, di- and tri- substituted linker during PFTR.....S28
 - 5.3.6. Figure S21 - Simulation for PFTR kinetic in case no equilibrium for the side reaction is considered.....S29

5.3.7. Figure S22 – SEC traces for the evolution of PFTR for PS2-SH in THF and DMF.....	S30
6. Optimized condition for PFTR (reactions performed with TCEP)	
6.1. Figure S23 – SEC traces for the investigation on the suppression of the side reaction.....	S31
6.2. Figure S24 – SEC traces for PFTR performed with a designed amount of TCEP.....	S32

Full characterization for PS1 and PS2 obtained *via* RAFT polymerization

Table S1 - Overview of the reactions and rate coefficients for PS1 and PS2 (monomer: styrene) with $I_2, I^{\bullet}, M, R_0^{\bullet}, R_i^{\bullet}, P_i, R_0X, R_iX$: conventional radical initiator, initiator fragment, monomer, RAFT leaving group, macroradical (chain length $i \geq 1$), dead polymer species, initial RAFT agent, dormant macrospecies; 70°C; for termination apparent rate coefficients with given value the one of $k_{t,app}^{1,1}$

Reaction	Equation	k ((L mol ⁻¹) s ⁻¹)	ref
Dissociation ^(a)	$I_2 \xrightarrow{f, k_{dis}} 2I^{\bullet}$	$4.4 \cdot 10^{-5}$	1
Chain Initiation	$I^{\bullet} + M \xrightarrow{k_{pI}} R_1^{\bullet}$	$5.2 \cdot 10^3$	2
	$R_0^{\bullet} + M \xrightarrow{k_{pR_0}} R_1^{\bullet}$	$5.2 \cdot 10^3$	2
Propagation	$R_i^{\bullet} + M \xrightarrow{k_p} R_{i+1}^{\bullet}$	$4.8 \cdot 10^2$	3
Termination by recombination	$R_0^{\bullet} + R_0^{\bullet} \xrightarrow{k_{tc,00}} P_0$	$2 \cdot 10^{8.7}$	4,5
	$R_0^{\bullet} + R_i^{\bullet} \xrightarrow{k_{tc,0}} P_i$	$2 \cdot 10^{8.7}$	4,5
	$R_i^{\bullet} + R_j^{\bullet} \xrightarrow{k_{tc,app}^{ij}} P_{i+j}$	$2 \cdot 10^{8.7}$	4,5
RAFT exchange		$3.3 \cdot 10^6$	
	$R_i^{\bullet} + R_0X \xrightleftharpoons[k_{frag,1}]{k_{add,1}} R_iXR_0 \xrightleftharpoons[k_{add,2}]{k_{frag,2}} R_iX + R_0^{\bullet}$	$3.5 \cdot 10^4$	6(b)
		$5.3 \cdot 10^5$	
		$5.7 \cdot 10^4$	
	$R_i^{\bullet} + R_jX \xrightleftharpoons[k_{frag}]{k_{add}} R_iXR_j \xrightleftharpoons[k_{add}]{k_{frag}} R_iX + R_j^{\bullet}$	$7.7 \cdot 10^4$	6(b)
		$9.6 \cdot 10^4$	

(a) (apparent) efficiency f , (b) values for CPDT instead of Dopat

- Erben, M. T. & Bywater, S. The thermal decomposition of 2,2'-Azo-bis-isobutyronitrile. Part I. Products of the Reaction. *J. Am. Chem. Soc.* **77**, 3712–3714 (1955).
- Heberger, K. & Fischer, H. Rate Constants for the Addition of the 2-Cyano-2-Propyl Radical Alkenes in Solution. *Int. J. Chem. Kinet.* **25**, 749–769 (1993).
- Buback, M. *et al.* Critically evaluated rate coefficients for free-radical Propagation rate coefficient for styrene. *Macromol. Chem. Phys.* **3280**, 3267–3280 (2006).
- Johnston-Hall, G. & Monteiro, M. J. Bimolecular Radical Termination: New Perspectives and Insights. *J. Polym. Sci. Part a-Polymer Chem.* **46**, 3155–3176 (2008).
- Derboven, P., D'hooge, D. R., Reyniers, M.-F., Marin, G. B. & Barner-Kowollik, C. The Long and the Short of Radical Polymerization. *Macromolecules ASAP* (2015). doi:10.1021/ma5017659
- Desmet, G.B., De Rybel, N., Van Steenberghe, P.H.M., D'hooge, D.R., Reyniers, M.F. & Marin, G.B. Ab-initio-based kinetic modeling to understand RAFT exchange: the case of 2-cyano-2-propyl dodecyl trithiocarbonate and styrene. *Macromolecular Rapid Communications.* (2017).

Section S1a - Apparent termination rate coefficient

In order to accurately describe the diffusion-controlled mechanism of bimolecular termination in radical polymerization, the composite k_t model⁴ (aka RAFT-CLD-T model) was used. This model allows to calculate an apparent homotermination rate coefficient ($k_{tc,app}^{i,i}$; i =chain length; only considering termination by recombination) dependent on the chain length i and the monomer conversion X_m :

For $i < i_{gel}$

$$k_{tc,app}^{i,i} = k_t^{1,1} i^{-\alpha_s} \quad \text{for } i < i_{SL}$$

$$k_{tc,app}^{i,i} = k_t^{1,1} i_{SL}^{(\alpha_L - \alpha_s)} i^{-\alpha_s} \quad \text{for } i \geq i_{SL}$$

For $i \geq i_{gel}$

$$k_{tc,app}^{i,i} = k_t^{1,1} i_{SL}^{(\alpha_{gel} - \alpha_s)} i^{-\alpha_{gel}} \quad \text{for } i < i_{SL}$$

$$k_{tc,app}^{i,i} = k_t^{1,1} i_{SL}^{(\alpha_L - \alpha_s)} i^{(\alpha_{gel} - \alpha_L)} i^{-\alpha_{gel}} \quad \text{for } i \geq i_{SL}$$

with $k_t^{1,1}$ the (apparent) termination rate coefficient for radicals with chain length 1, α_s the exponent for termination of short chains in dilute solution, α_L the exponent for long chains in dilute solution, α_{gel} the exponent for chains in the gel regime, i_{SL} the crossover chain length between short- and long-chain behavior, i_{gel} the chain length at the onset of the gel-effect. An overview of these parameters can be found in Table S2.⁴

From the apparent homotermination rate coefficients, the apparent cross-termination rate coefficient $k_{tc,app}^{i,j}$ is calculated for simplicity using the geometric mean:

$$k_{tc,app}^{i,j} = \sqrt{k_{tc,app}^{i,i} k_{tc,app}^{j,j}}$$

An averaged (zero order) apparent termination rate coefficient can be calculated at any moment:

$$\langle k_{tc,app} \rangle = \frac{\sum_{i=1}^{\infty} \sum_{j=1}^{\infty} k_{tc,app}^{i,j} [R_i][R_j]}{(\sum_{i=1}^{\infty} [R_i])^2}$$

Table S2 - Parameters used for the composite k_t model⁴

Monomer	T(K)	$k_t^{1,1}$	α_s	i_{SL}	α_L	α_{gel}	i_{gel}
Sty	363	$2 \times 10^{8.7}$	0.53	30	0.15	$1.22X_m - 0.11$	$3.30X_m^{-2.13}$

Section S1b - Apparent conventional initiator efficiency

An apparent conventional initiator efficiency f_{app} dependent on monomer conversion X_m can be calculated as described by Buback *et.al.*:⁷

$$f_{app} = \frac{D_I}{D_I + D_{term}} \quad (S1)$$

with D_I the diffusion coefficient of the cyanoisopropyl radical and $D_{term} = 5.3 \cdot 10^{-10} \text{m}^2 \text{s}^{-1}$ a correction factor related to the rate of termination between two cyanoisopropyl radicals.

According to the free volume theory, D_I can be calculated via:

$$D_I = D_{0,I} \exp\left(-\frac{E_I}{RT}\right) \exp\left(\frac{-w_1 V_1^* \xi_{i2} / \xi_{12} + w_2 V_2^* \xi_{12}}{V_{FH} / \lambda}\right)$$

$$\frac{V_{FH}}{\lambda} = \frac{K_{11}}{\lambda} w_1 (K_{21} - T - T_{g1}) + \frac{K_{12}}{\lambda} w_2 (K_{22} + T - T_{g1})$$

Table S3 gives an overview of the description and value of the parameters used.

Table S3 - Parameters used to calculate the apparent initiator efficiency as described by Buback et al. for AIBN as conventional radical initiator and styrene as monomer

Parameter	Description	Value
$D_{0,I} (\text{m}^2 \text{s}^{-1})$	Pre-exponential factor for diffusion	$1.95 \cdot 10^{-4}$
$E_I (\text{kJ mol}^{-1})$	Activation energy for diffusion	31
$R (\text{J mol}^{-1} \text{K}^{-1})$	Universal gas constant	8.314
$T (\text{K})$	Temperature	333 – 363
$w_1 (-)$	Mass fraction of monomer	0-1
$w_2 (-)$	Mass fraction of polymer	0-1
$V_1^* (\text{m}^3 \text{mol}^{-1})$	Specific critical hole free volume of monomer ^(a)	$9.46 \cdot 10^{-7}$
$V_2^* (\text{m}^3 \text{mol}^{-1})$	Specific critical hole free volume of polystyrene	$8,50 \cdot 10^{-7}$
$\frac{K_{11}}{\lambda} (\text{m}^3 \text{kg}^{-1} \text{K}^{-1})$	Parameter for specific hole free volume monomer ^(a)	$1.49 \cdot 10^{-9}$
$\frac{K_{12}}{\lambda} (\text{m}^3 \text{kg}^{-1} \text{K}^{-1})$	Parameter for specific hole free volume polymer	$5.82 \cdot 10^{-10}$
$K_{21} - T_{g1} (\text{K})$	Parameter for specific hole free volume monomer ^(a)	-84
$K_{22} - T_{g1} (\text{K})$	Parameter for specific hole free volume polymer	-327
$\xi_{i2} (-)$	Critical jumping unit volume ratio for cyanoisopropyl radical to polymer	0.36
$\xi_{12} (-)$	Critical jumping unit volume ratio for monomer to polymer	0.59

7. Buback, M., Huckestein, B., Kuchta, F. & Russell, G. T. Initiator efficiencies in 2,2'-azoisobutyronitrile-initiated freeradical polymerizations of styrene. *Macromol. Chem. Phys.* **2140**, 2117–2140 (1994).

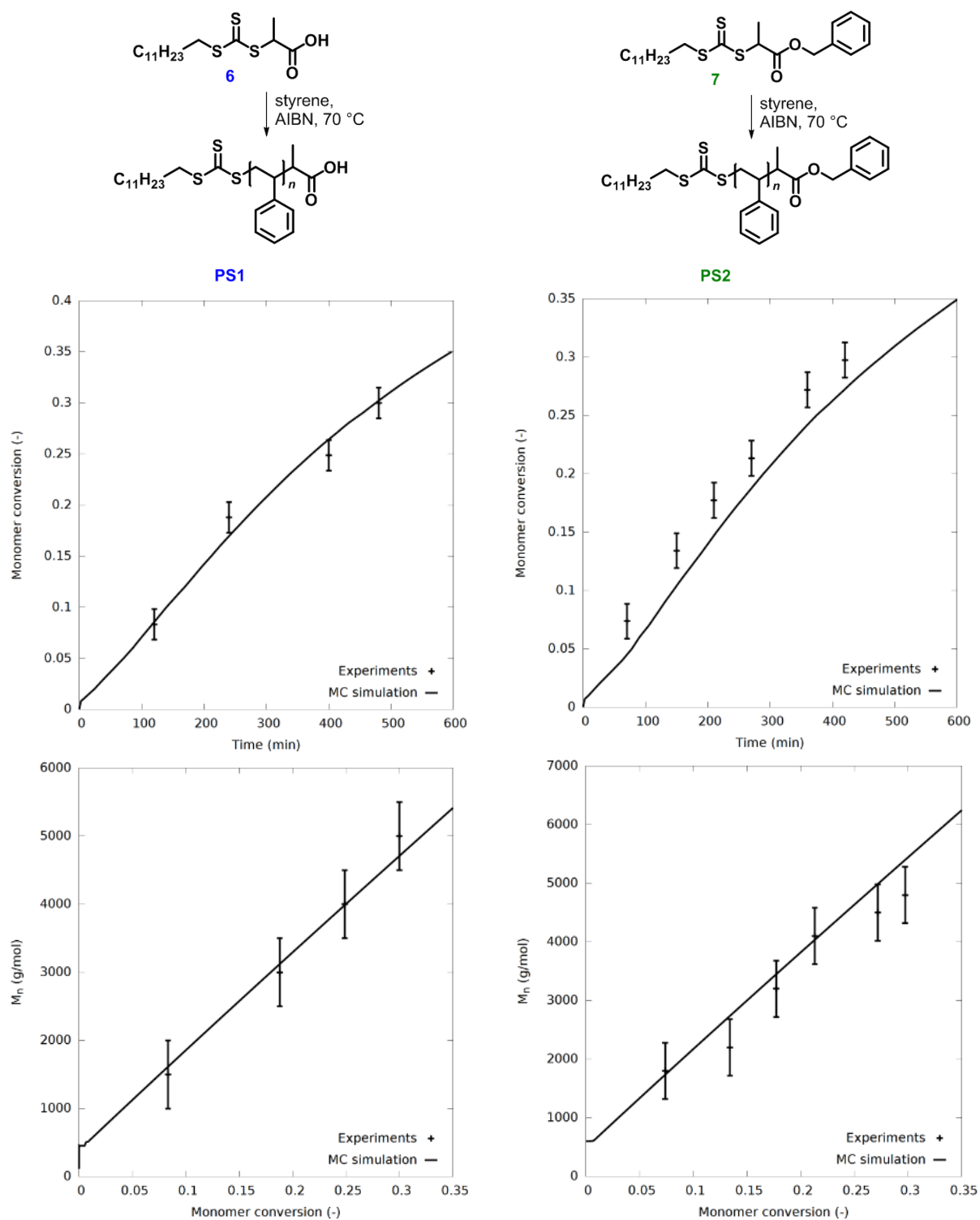


Figure S1 – Top: Schematic representation of the polymerization simulated PS1 (left) or PS2 (right). Middle and Bottom: *k*MCS simulations for RAFT polymerization kinetic for PS1 (left) and PS2 (right).

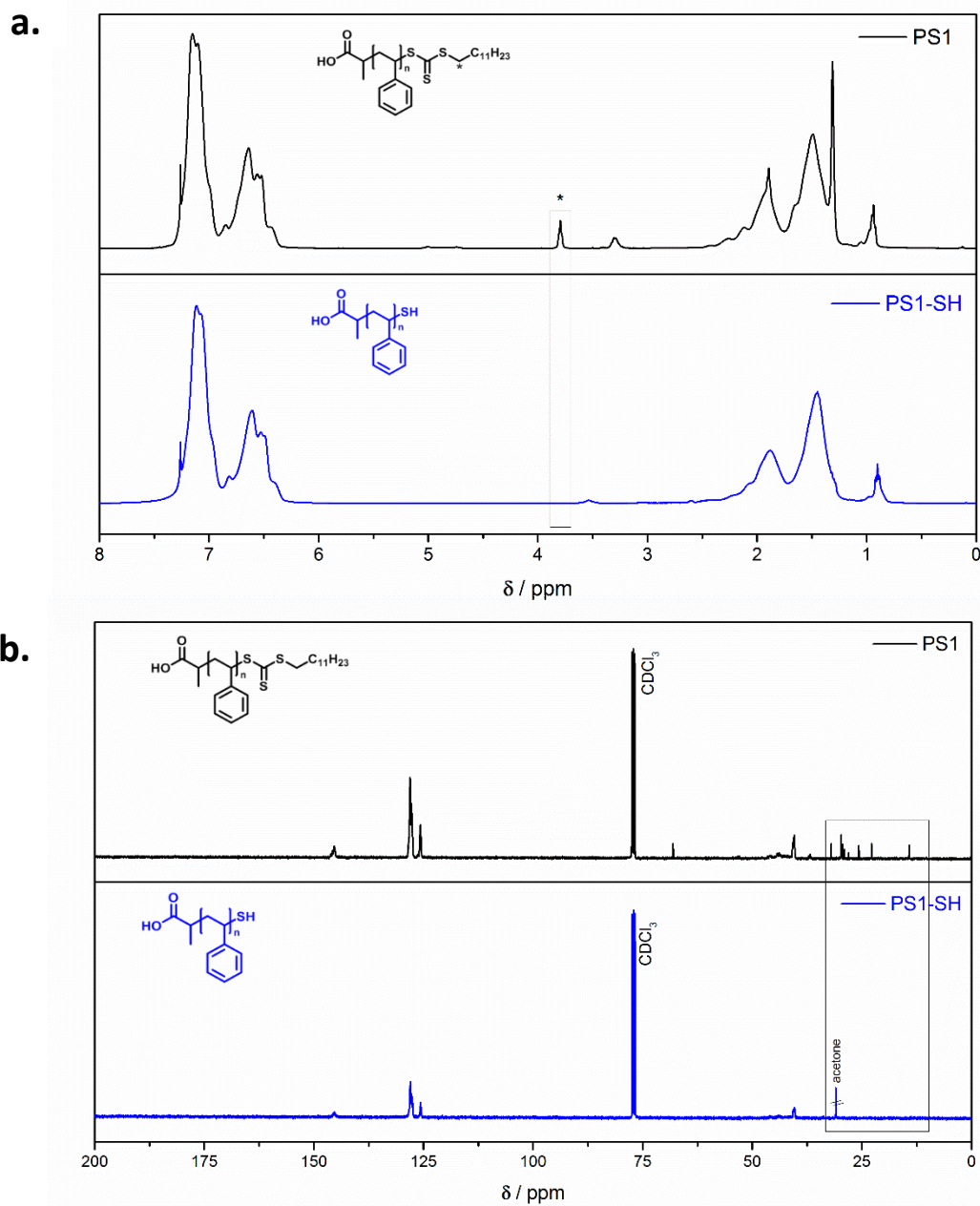


Figure S2 – Full characterization *via* NMR of PS1 before (black) and after (blue) aminolysis. **a.** $^1\text{H-NMR}$ (CDCl₃, 400 MHz) Highlighted in the box the disappearance of the –CH₂– marked in the structure. $\delta = 7.50 - 6.20$ (m, ArH), $3.0 - 0.50$ (m, aliphatic H), $2.50 - 0.84$ ppm (m, aliphatic H). **b.** $^{13}\text{C-NMR}$ (CDCl₃, 100 MHz) spectrum of PS1 before and after aminolysis (PS1 and PS1-SH). Highlighted in the box the disappearance of the resonances corresponding to the aliphatic carbon chain of the RAFT agent. $\delta = 145.43$ (C, quaternary carbon in the styrene aromatic ring), 128.33 and 125.52 (-HC=CH-, unsaturated carbons, styrene ring), and 40.30 (aliphatic C, aliphatic polymer backbone).

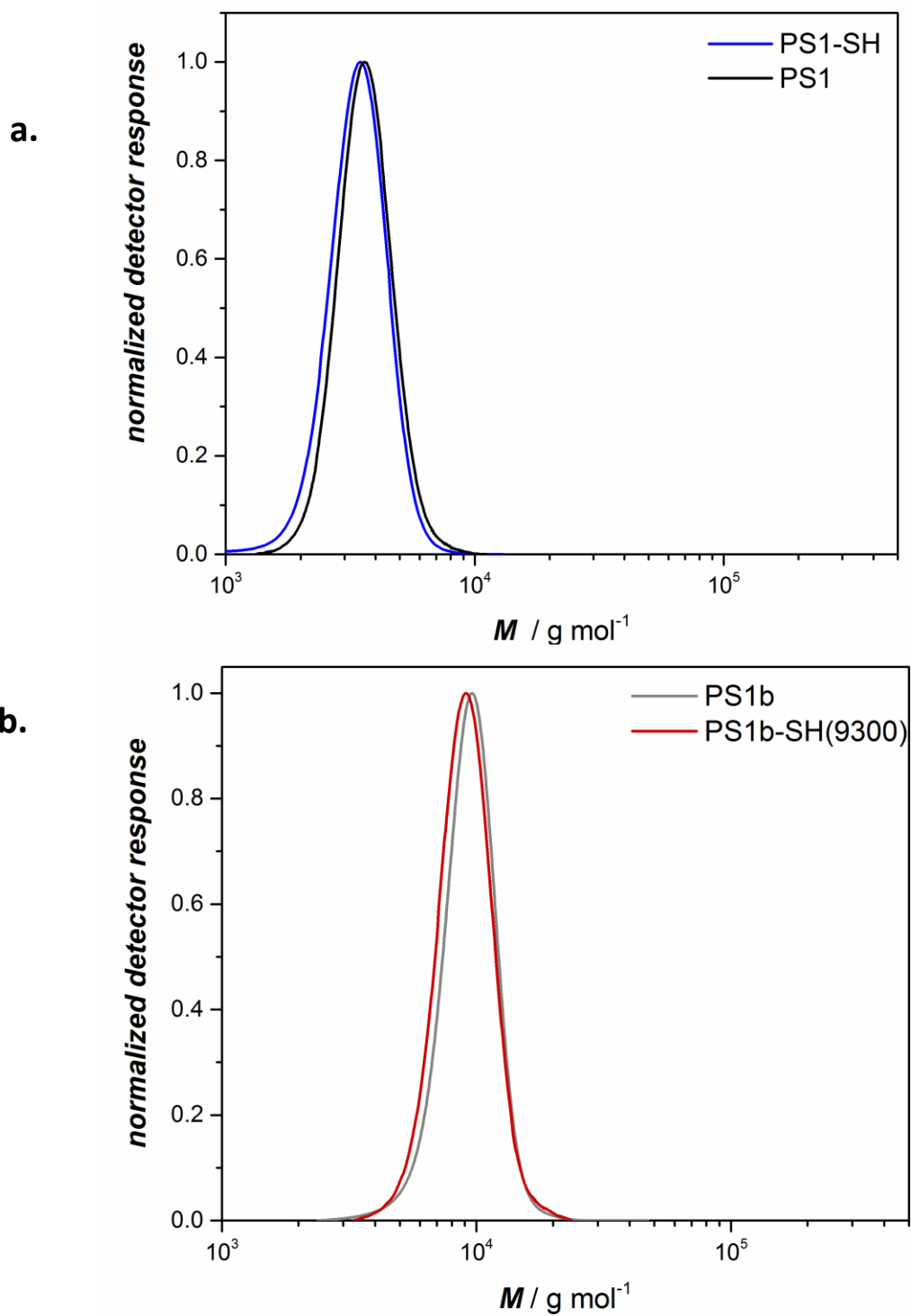


Figure S3 - SEC traces for **a.** PS1 (black) and PS1-SH (blue) and **b.** PS1b (gray) and PS1b-SH(9300) (red).

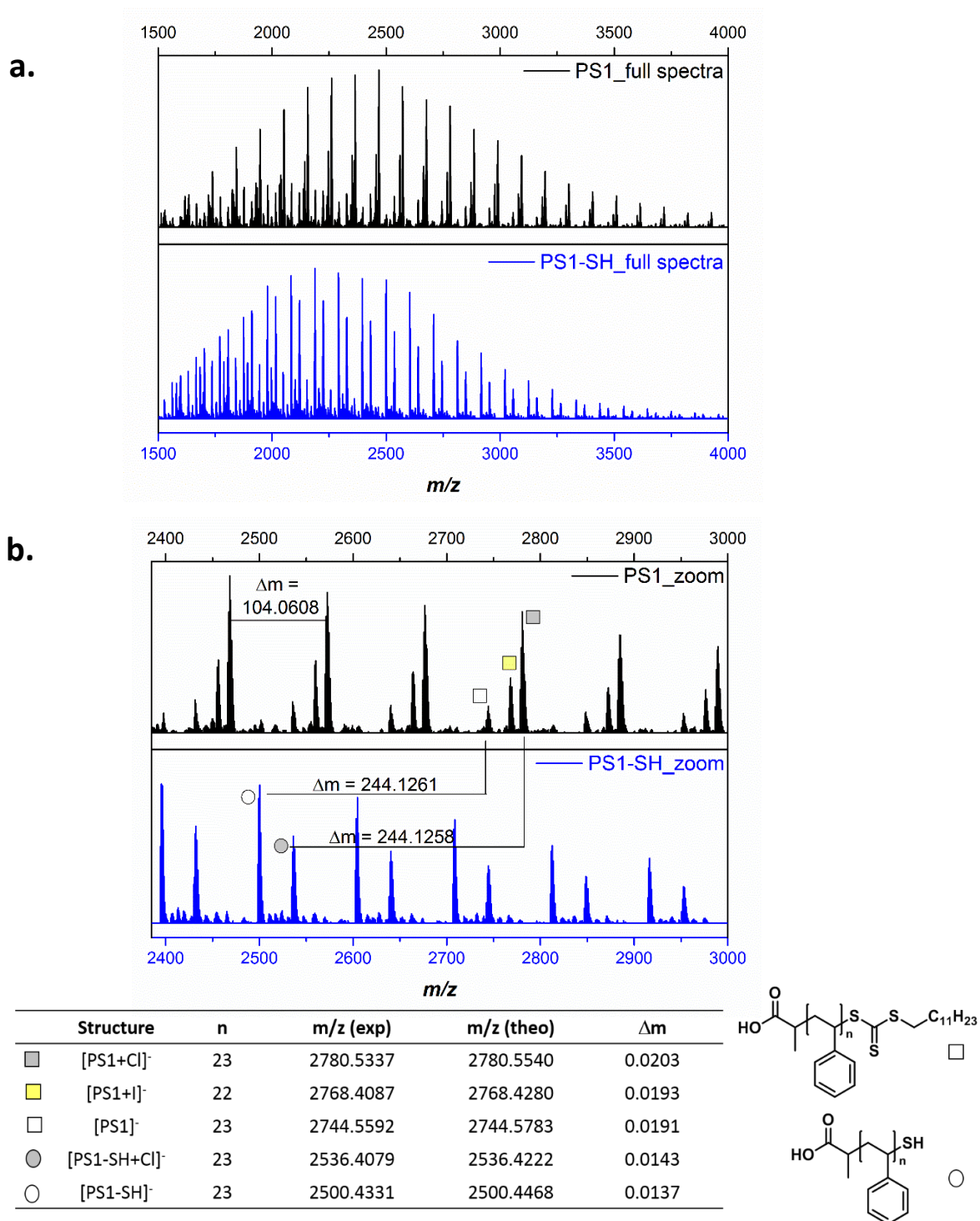


Figure S4 - ESI-MS spectra recorded in negative mode for PS1 (black) and PS1-SH (blue). **a.** full spectra recorded in the range $m/z = 1500-4000$, **b.** representative zoom in order to identify the species. The assignments are listed in the associated table and in agreement with the proposed structure before (square) and after (circle) aminolysis, within the same spectra $\Delta m = 104$ corresponding to the styrene unit, between the two spectra $\Delta m = 244$ corresponding to the loss of the aliphatic chain and the trithiocarbonate removed from the parent PS1.

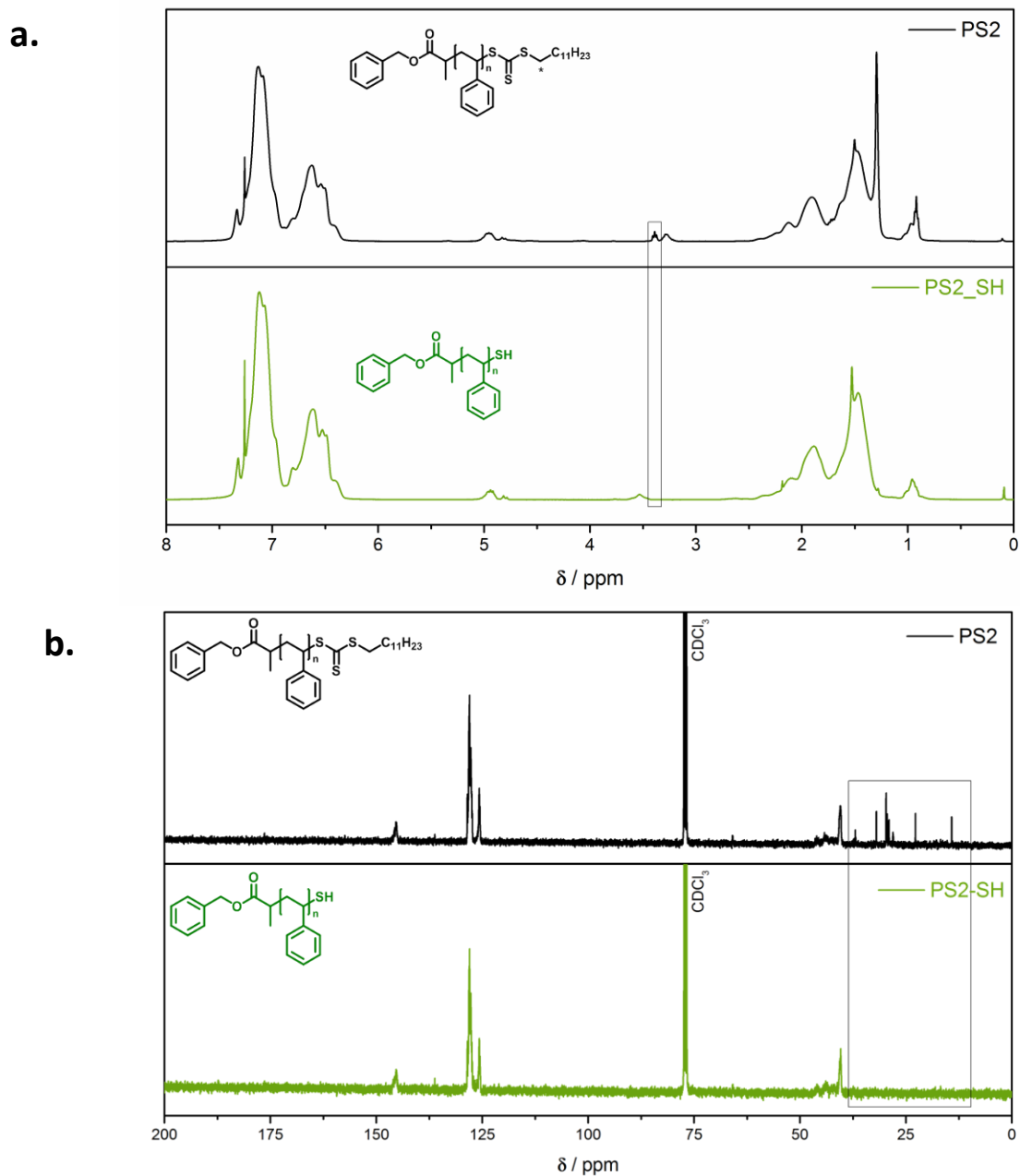


Figure S5 - Full characterization via NMR of PS1 before (black) and after (blue) aminolysis. **a.** $^1\text{H-NMR}$ (CDCl_3 , 400 MHz) Highlighted in the box the disappearance of the $-\text{CH}_2-$ marked in the structure. $\delta = 7.50 - 6.20$ (m, ArH), $2.5 - 0.50$ (m, aliphatic H), $2.50 - 0.84$ ppm (m, aliphatic H). **b.** $^{13}\text{C-NMR}$ (CDCl_3 , 100 MHz) spectrum of PS1 before and after aminolysis (PS1 and PS1-SH). Highlighted in the box the disappearance of the resonances corresponding to the aliphatic carbon chain of the RAFT agent. $\delta = 145.43$ (C, quaternary carbon in the styrene aromatic ring), $\delta = 128.33$ and $\delta = 125.52$ ($-\text{HC}=\text{CH}-$, unsaturated carbons, styrene ring), and $\delta = 40.30$ (aliphatic C, aliphatic polymer backbone).

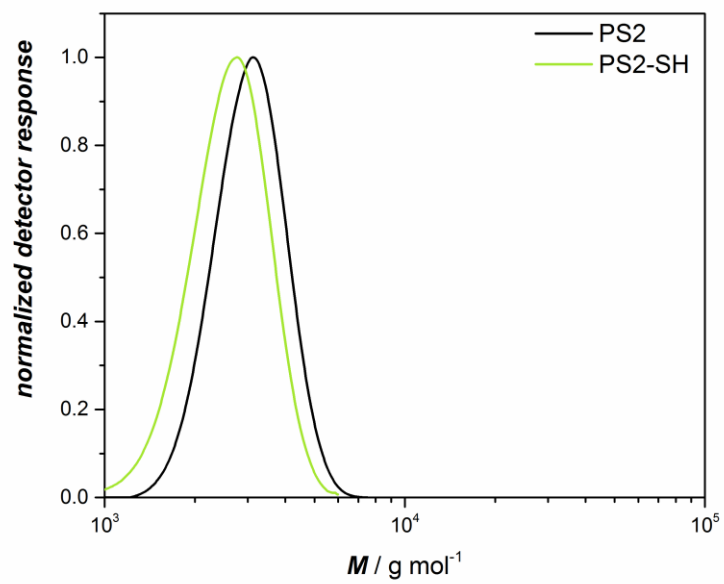


Figure S6 - SEC traces for PS2 (black) and PS2-SH (green).

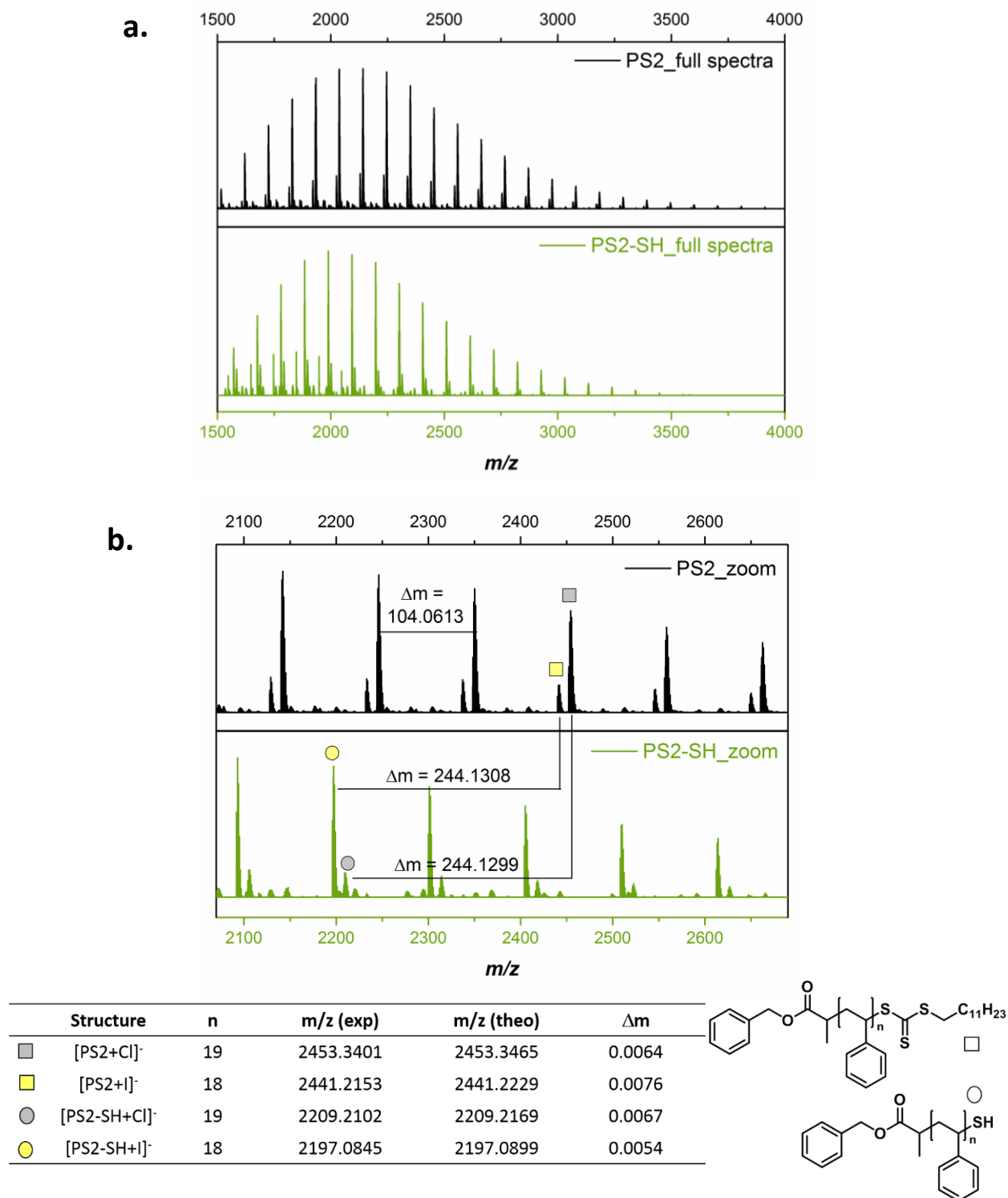


Figure S7 - ESI-MS spectra recorded in negative mode for PS2 (black) and PS2-SH (green). a. full spectra recorded in the range $m/z = 1500-4000$, b. representative zoom in order to identify the species. The assignments are listed in the associated table and in agreement with the proposed structure before (square) and after (circle) aminolysis. Within the same spectra $\Delta m = 104$ corresponding to the styrene unit, between the two spectra $\Delta m = 244$ corresponding to the loss of the aliphatic chain and the trithiocarbonate removed from PS1.

Characterization of 2,3,4,5,6-pentafluorobenzyl benzoate (1PFB)

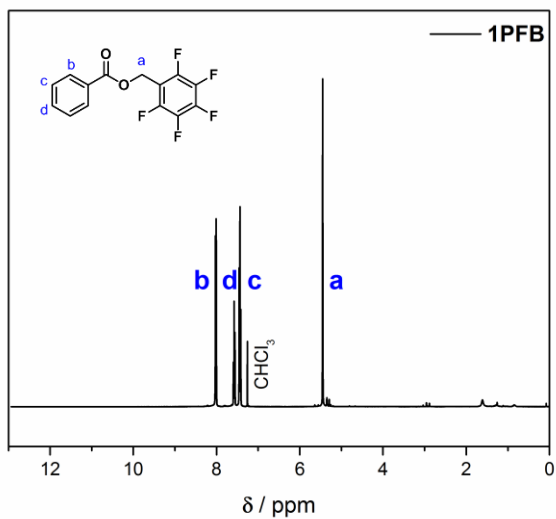


Figure S8 - ¹H-NMR spectrum (400 MHz, CDCl₃) of 1PFB. δ = 5.45 (s, 2H, CH₂), 7.44 (dt, 2H, CH), 7.58 (tt, 1H, CH), 8.00 (td, 1H, CH).

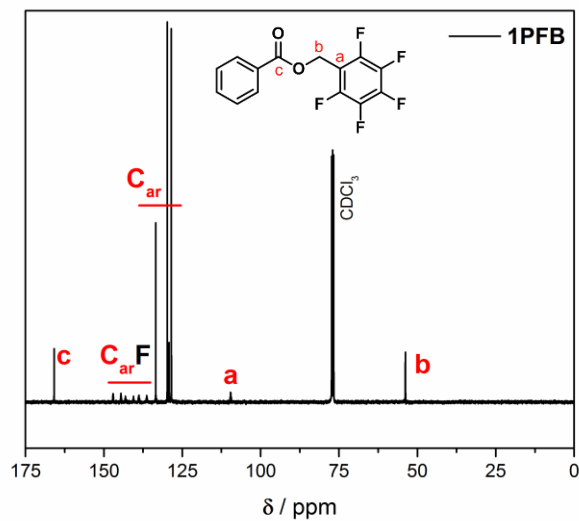


Figure S9 - ¹³C-NMR spectrum (100 MHz, CDCl₃) of 1PFB. δ = 55.83 (1C, aliphatic CH₂), δ = 109.59 (1C, C aromatic ring), δ = 128-134 (6C, C aromatic ring), 137-147 (6C, aromatic fluorinated ring), 165.86 (1C, ester).

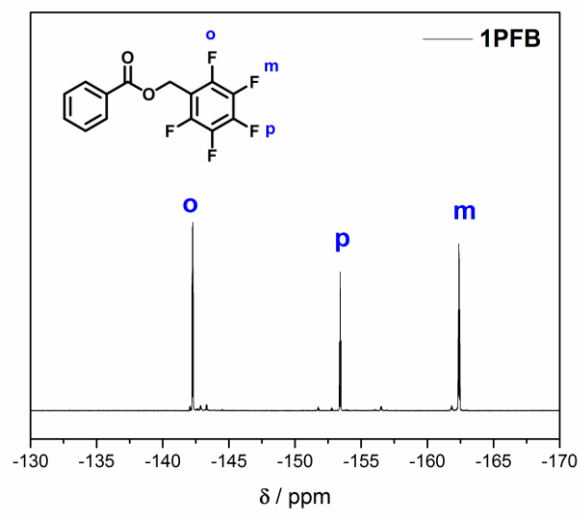


Figure S10 - ^{19}F -NMR spectrum (CDCl_3 , 376 MHz) of 1PFB. $\delta = -142.2$ (ortho), $\delta = -153.4$ (para), $\delta = -162.4$ (meta).

NMR spectroscopy and determination of the PFB conversion via ^{19}F -NMR measurements

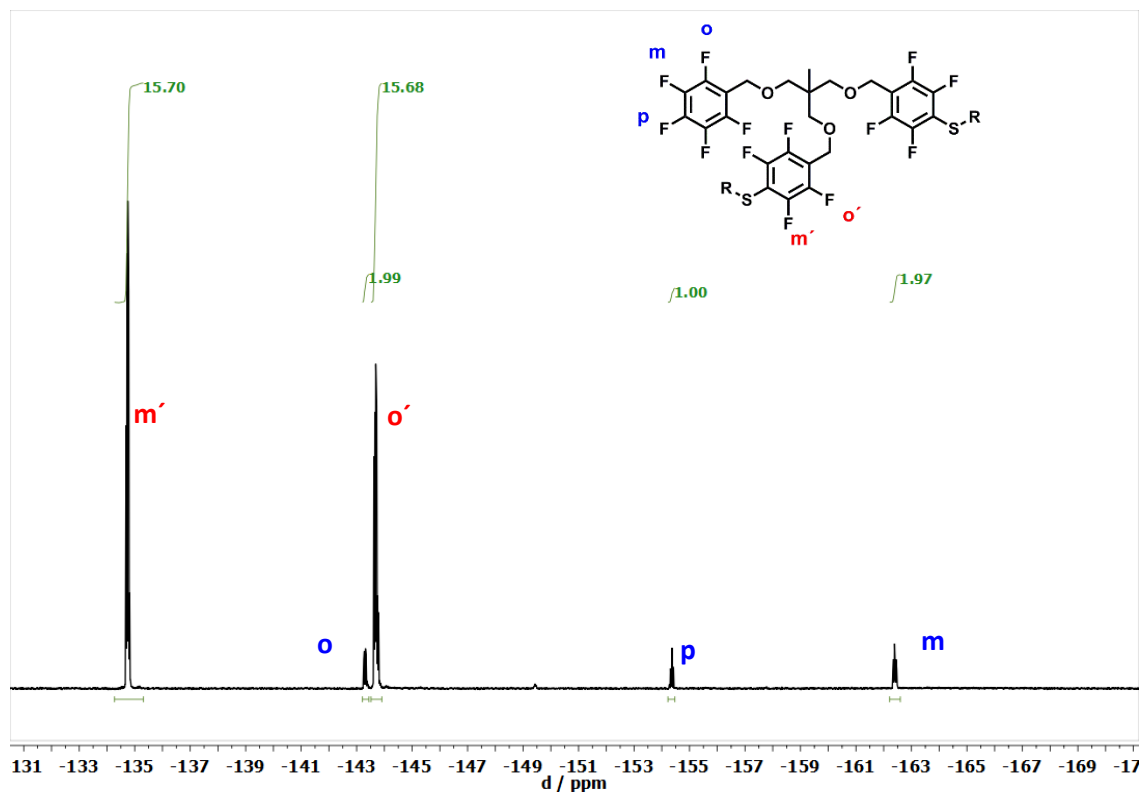


Figure S11 - Representative ^{19}F -NMR spectrum (376MHz, CDCl_3) of a selected sample from the kinetic study. Calculation of the conversion via ^{19}F -NMR.

$$\text{conversion} = 1 - \frac{1}{1 + \left(\frac{15.69}{2}\right)} = 0.89 * 100 = 89 \%$$

Table S4 - Summary of all the reaction conditions discussed for the investigation of disulfide bond formation (side reaction)

		Disulphide (no PFB linker)							
		1	2	3	4	5	PS1-SH (3800)	PS2-SH (2800)	
without TCEP	SH:DBU 1:1	150mM THF		150mM THF				Fig. 3	Table 2
		Fig. S13		Fig. 2a			75mM THF/DMF	75mM THF/DMF	
With TCEP	SH:DBU 1:15						37mM DMF, O ₂		
							37mM DMF, Argon	Fig. S23	
							37mM DMF, O ₂ SH:TCEP = 1:6		
							37mM DMF, Argon SH:TCEP = 1:6		
							37mM DMF, Argon SH:TCEP = 1:4	Fig. 7b	
							37mM DMF, Argon SH:TCEP = 1:2		
					37mM DMF, Argon SH:TCEP = 1:1				
					37mM DMF, Argon SH:TCEP = 1:0.5				

Table S5 - Summary of all the reaction conditions discussed for the investigation of PFTR reaction (main reaction)

		PFTR (with PFB linker)*							
		SH:PFB group = 1:1, always							
		1	2	3	4	5	PS1-SH (3800)	PS1b-SH (9300)	PS2-SH (2800)
without TCEP	SH:DBU 1:1	75mM THF	75mM THF	75mM THF	75mM THF	75mM THF/DMF	75mM THF/DMF	-	75mM THF/DMF
				Fig. S13			75mM THF/DMF (1PFB)	Fig. 3c,d	Fig. 5
							75mM DMF	75mM DMF	Fig. 6
with TCEP	SH:DBU 1:15						37mM DMF		
							37mM DMF SH:TCEP = 1:1		
						37mM DMF SH:TCEP = 1:6			

Fig. 7

*PFB linker is meant as 3PFB, unless differently specified in the table

Kinetic modelling

Section S5a - SEC broadening

1) SEC broadening small molecule system



SEC broadening is accounted for by introducing a normal distribution on log scale with standard deviation $\sigma_{thiol} = \sigma_{disulphide} = 0.03$ in both THF and DMF.

2) SEC broadening polymer system

For a polymer system, there are two contribution to take into account for SEC broadening:

$$\sigma_{tot}^2 = \sigma_{reac}^2 + \sigma_{SEC}^2$$

- $\sigma_{reaction}$: already incorporated in the simulation

- σ_{SEC} : incorporated via the following equation:

$$w_{SEC}(\log M) = \frac{1}{(2\pi)^{0.5}\sigma_2} \int_0^{+\infty} \exp\left(-\frac{(\log(M) - \log(\tilde{M}))^2}{2\sigma_2^2}\right) w(\log \tilde{M}) d\log(\tilde{M})$$

In which $\sigma_2 = 0.06$ is determined for the polystyrene standards used in the GPC (see Figure below).

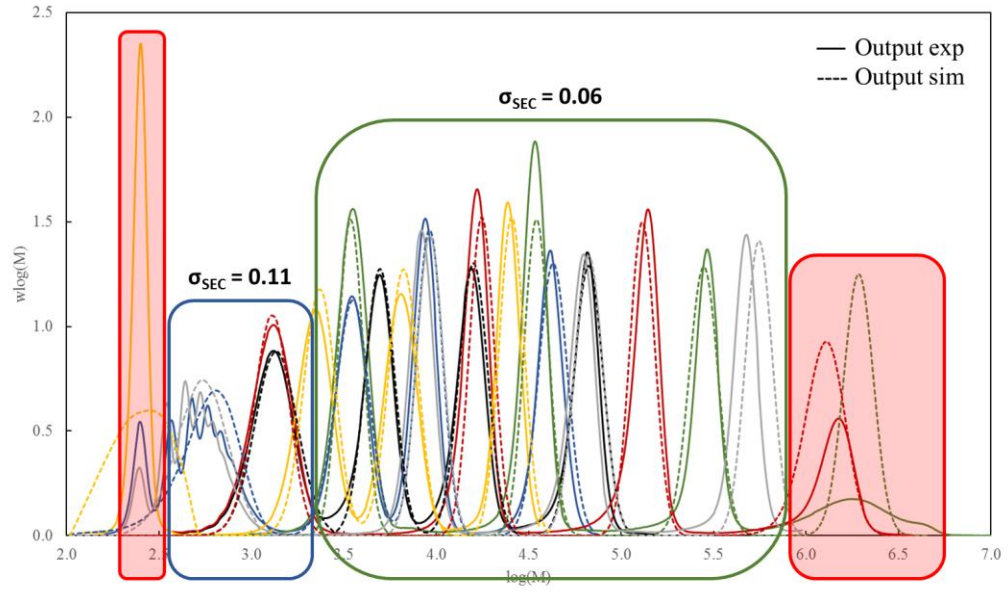
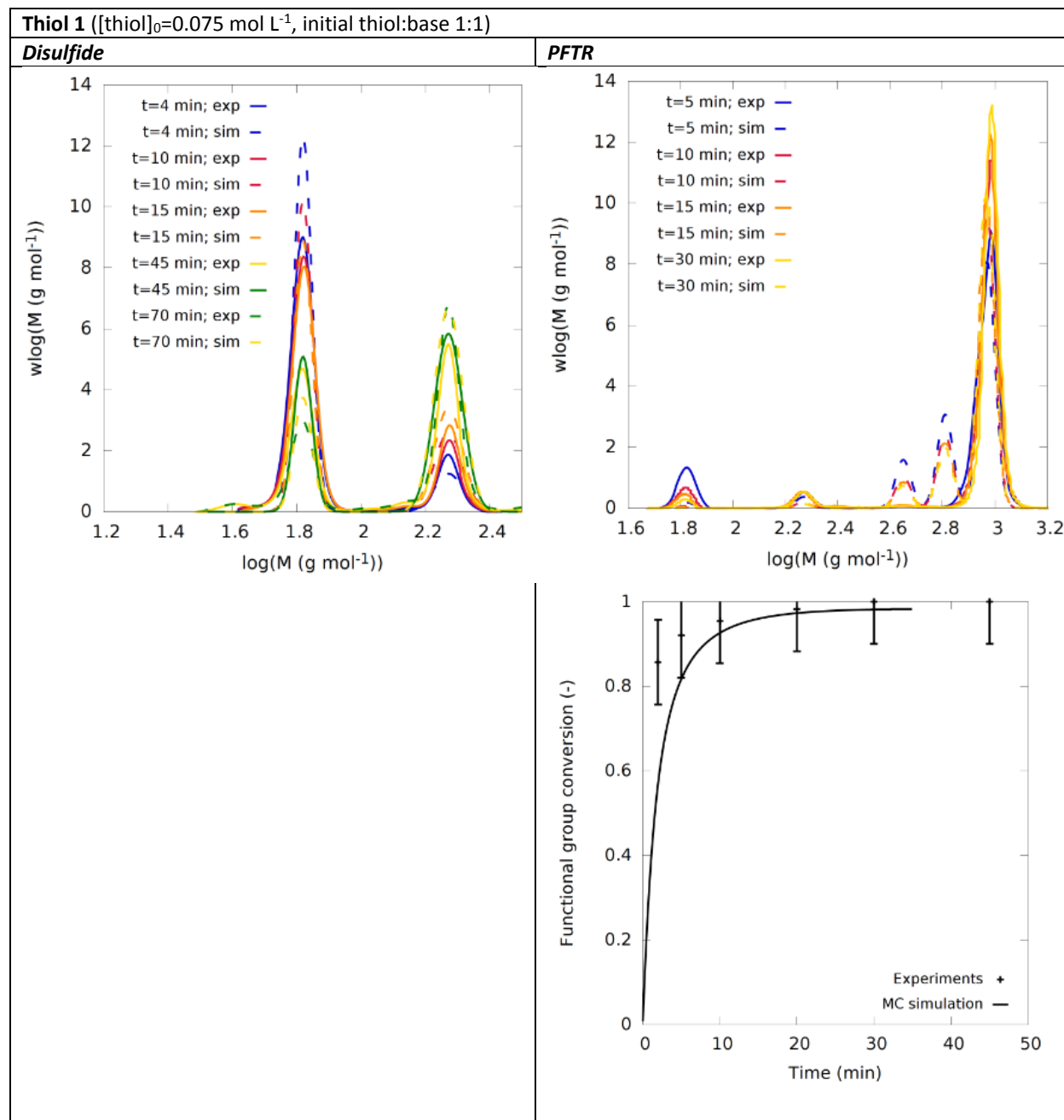


Figure S12 - SEC broadening PS standards.

PFTR and disulfide reaction for small thiol derivatives



Thiol 2 ([thiol] ₀ =0.075 mol L ⁻¹ , initial thiol:base 1:1)																									
Disulfide	PFTR																								
	<p>Functional group conversion (-)</p> <p>Time (min)</p> <p>Experiments + MC simulation —</p> <table border="1"> <caption>Approximate data for Thiol 2</caption> <thead> <tr> <th>Time (min)</th> <th>Functional group conversion (-)</th> </tr> </thead> <tbody> <tr><td>0</td><td>0.00</td></tr> <tr><td>1</td><td>0.30</td></tr> <tr><td>2</td><td>0.40</td></tr> <tr><td>3</td><td>0.60</td></tr> <tr><td>4</td><td>0.70</td></tr> <tr><td>7</td><td>0.85</td></tr> <tr><td>10</td><td>0.90</td></tr> <tr><td>15</td><td>0.95</td></tr> <tr><td>20</td><td>0.98</td></tr> <tr><td>30</td><td>0.99</td></tr> </tbody> </table>	Time (min)	Functional group conversion (-)	0	0.00	1	0.30	2	0.40	3	0.60	4	0.70	7	0.85	10	0.90	15	0.95	20	0.98	30	0.99		
Time (min)	Functional group conversion (-)																								
0	0.00																								
1	0.30																								
2	0.40																								
3	0.60																								
4	0.70																								
7	0.85																								
10	0.90																								
15	0.95																								
20	0.98																								
30	0.99																								
Thiol 4 ([thiol] ₀ =0.075 mol L ⁻¹ , initial thiol:base 1:1)																									
Disulfide	PFTR																								
	<p>Functional group conversion (-)</p> <p>Time (min)</p> <p>Experiments + MC simulation —</p> <table border="1"> <caption>Approximate data for Thiol 4</caption> <thead> <tr> <th>Time (min)</th> <th>Functional group conversion (-)</th> </tr> </thead> <tbody> <tr><td>0</td><td>0.00</td></tr> <tr><td>10</td><td>0.10</td></tr> <tr><td>20</td><td>0.20</td></tr> <tr><td>30</td><td>0.25</td></tr> <tr><td>40</td><td>0.35</td></tr> <tr><td>50</td><td>0.40</td></tr> <tr><td>70</td><td>0.45</td></tr> <tr><td>100</td><td>0.55</td></tr> <tr><td>120</td><td>0.60</td></tr> <tr><td>140</td><td>0.65</td></tr> <tr><td>250</td><td>0.80</td></tr> </tbody> </table>	Time (min)	Functional group conversion (-)	0	0.00	10	0.10	20	0.20	30	0.25	40	0.35	50	0.40	70	0.45	100	0.55	120	0.60	140	0.65	250	0.80
Time (min)	Functional group conversion (-)																								
0	0.00																								
10	0.10																								
20	0.20																								
30	0.25																								
40	0.35																								
50	0.40																								
70	0.45																								
100	0.55																								
120	0.60																								
140	0.65																								
250	0.80																								

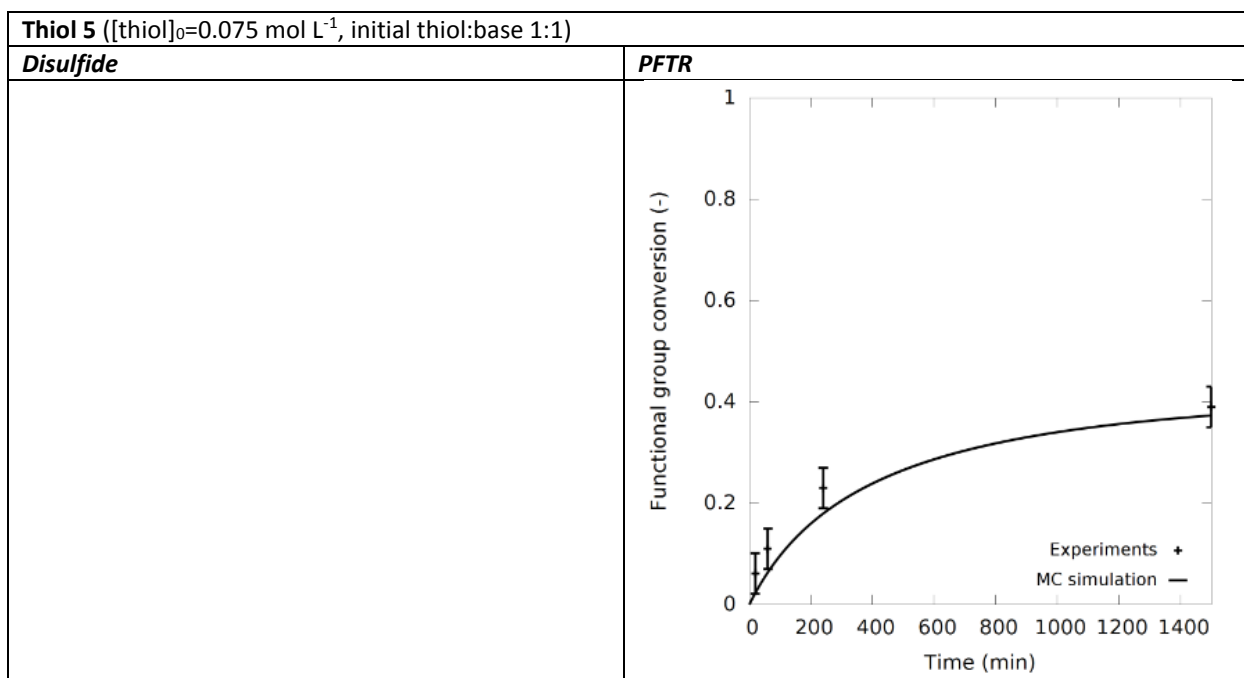
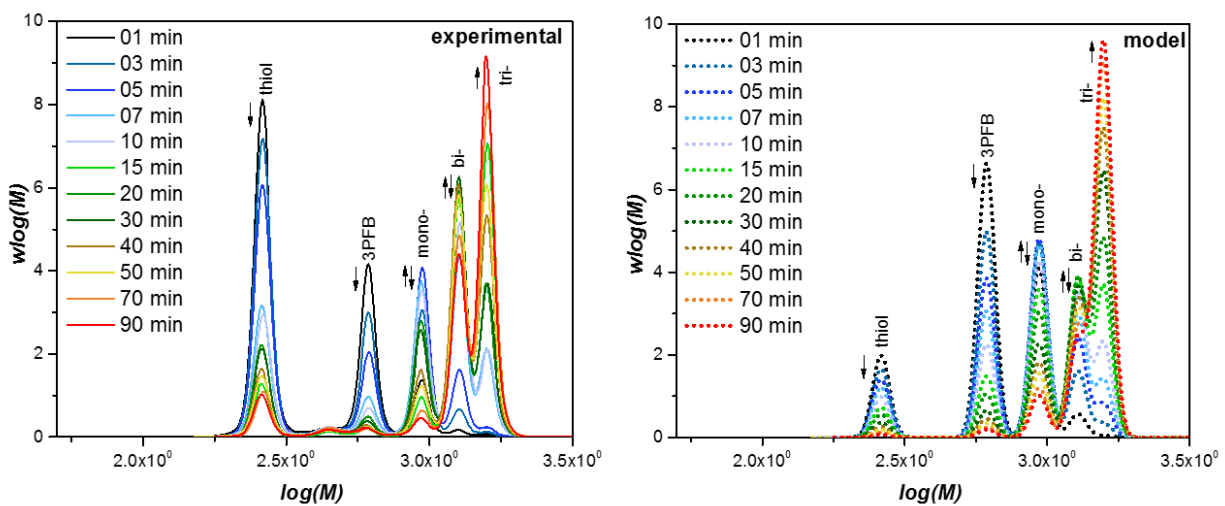


Figure S13 - Main results for kinetic studies of small molar mass thiol derivatives other than thiol **3** in THF. The adopted working conditions are specified in the figure.

a.



b.

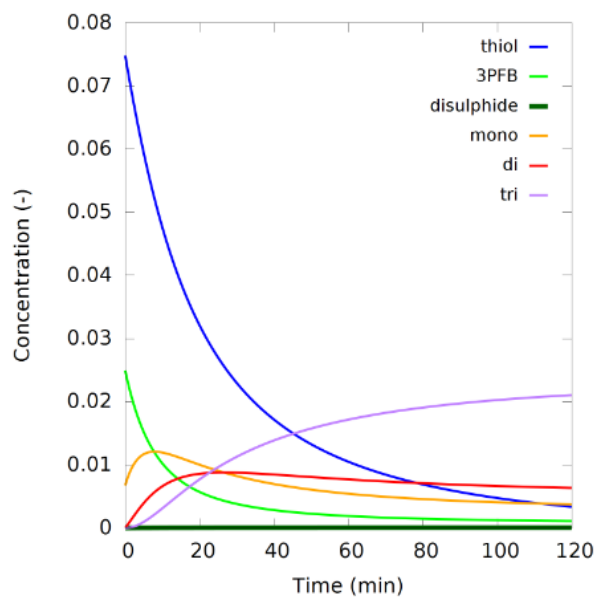


Figure S14 – a. experimental (left) and simulated (right) SEC traces at any reaction time for thiol **3** during PFTR (including the missing traces in Fig.2 of the main text). b. Simulated product spectrum (absolute concentrations) related to thiol **3** during PFTR.

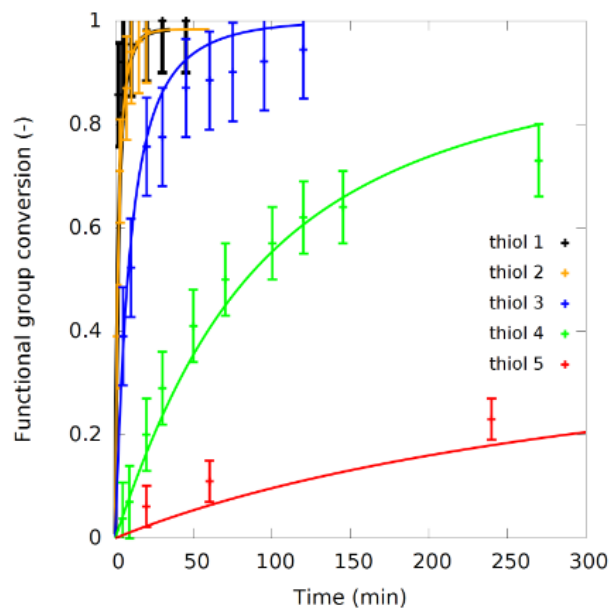


Figure S15 - Comparison of the PFTR kinetic for small molar mass thiol derivatives; thiol **1** (black), **2** (orange), **3** (blue), **4** (green) and **5** (red). All the kinetic were performed in THF, $[\text{thiol}]_0 = 0.075 \text{ molL}^{-1}$ and a ratio of $[\text{SH}]:[\text{PFB}]:[\text{DBU}] = 1:1:1$

Investigation on PFTR and disulfide bond formation for polymer system

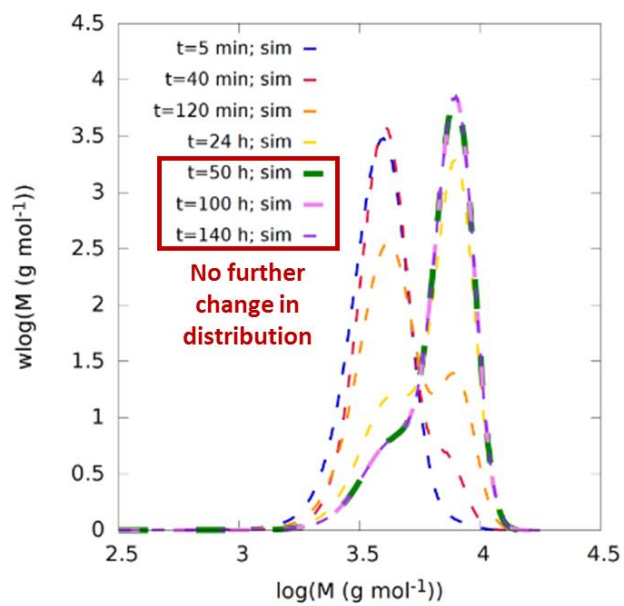


Figure S16 - Equilibrium reaction for disulfide formation in DMF.

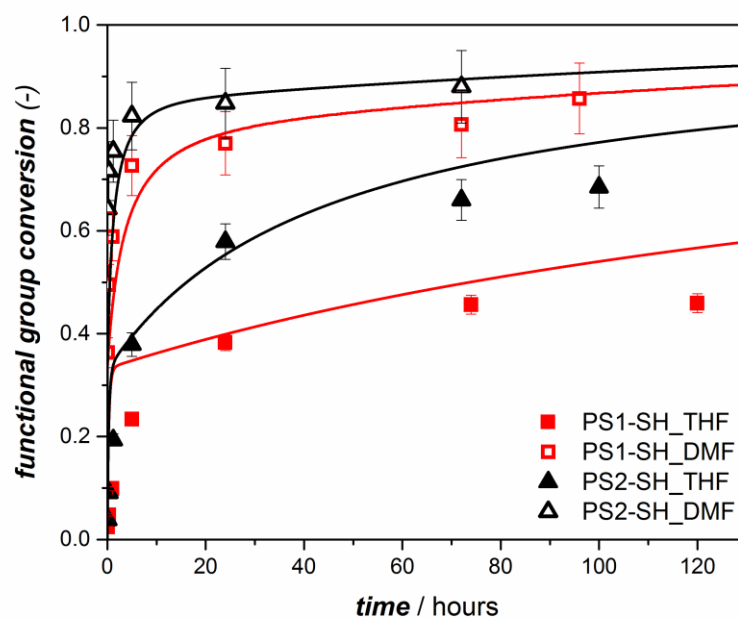


Figure S17 -Full kinetic, express as amount of PFB group reacted over time for PS1-SH (square, red) and PS2-SH (triangle, black). The kinetics are performed at ambient temperature $[\text{thiol}]_0 = 75\text{mM}$ using both THF (filled symbols) and DMF (empty symbols) as a solvent. The full line represent the relative fitting obtained via *kMC* simulation.

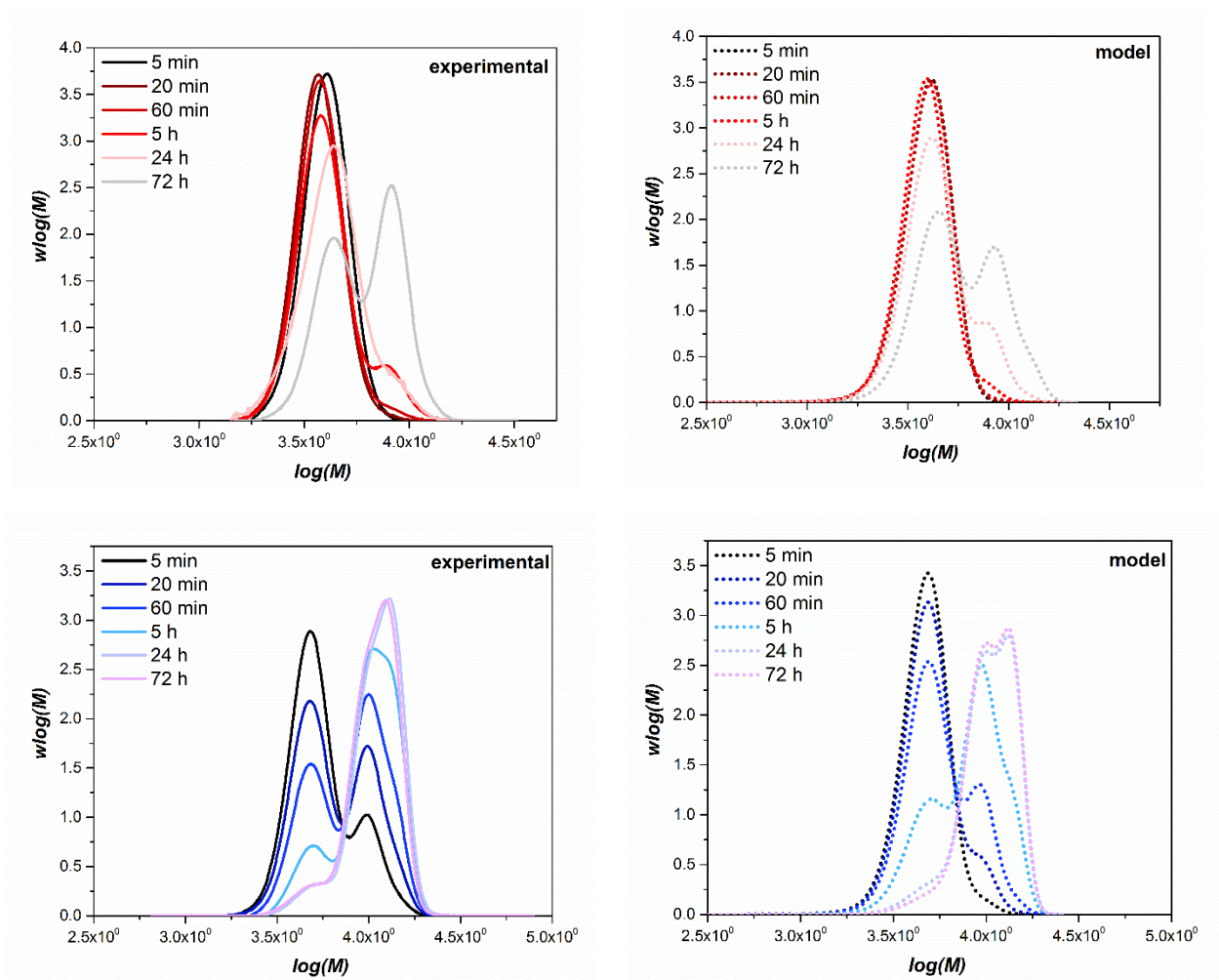


Figure S18 - SEC traces showing the evolution of PFTR employing 3PFB and PS1 in THF (red) and DMF (blue), $[\text{thiol}]_0 = 0.075 \text{ molL}^{-1}$ and SH:base = 1:1; (left) experimental data and (right) simulated data.

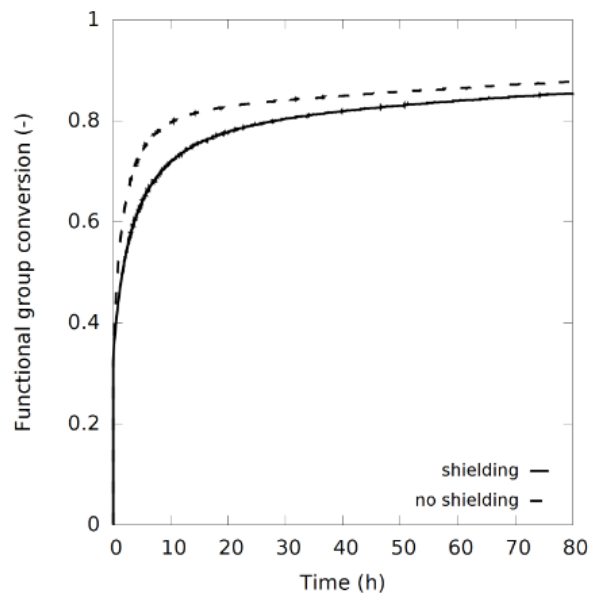


Figure S19 - PFB conversion (-) vs. time (h) for PS1-SH in case $f_{\text{shielding}}=1/S.D.$ (full line) and in case $f_{\text{shielding}}=1$ (dashed line) (thiol:DBU = 1:1, $[\text{thiol}]_0 = 0.075 \text{ mol L}^{-1}$).

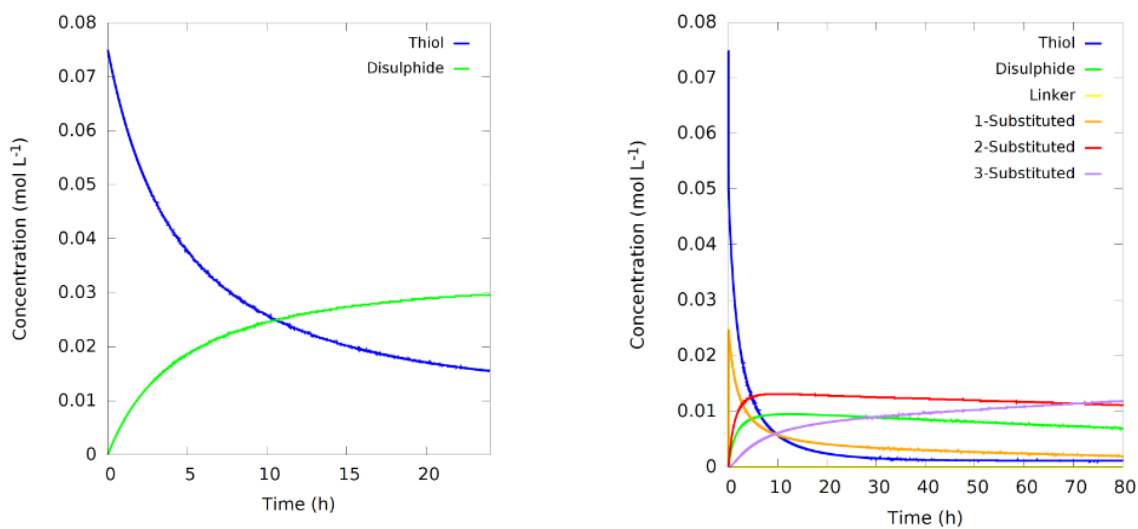


Figure S20 - Concentrations of the different reaction components (mol L^{-1}) vs. time (h) ($[\text{thiol}]_0 = 0.075 \text{ mol L}^{-1}$) (left) in absence of 3PFB linker and (right) in presence of 3 PFB linker.

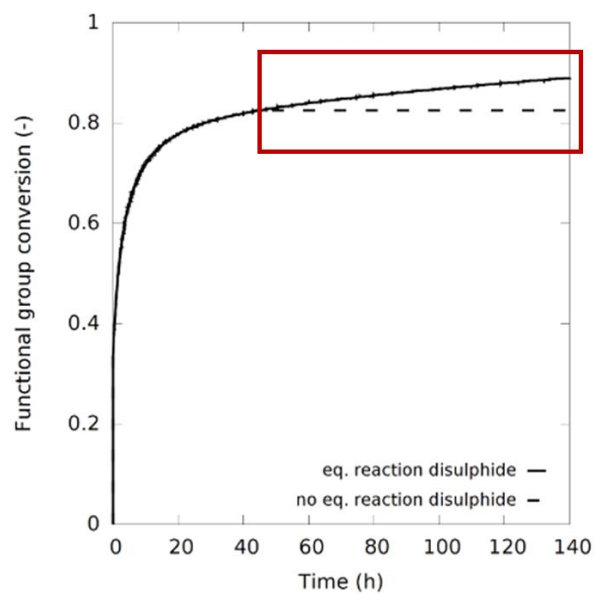


Figure S21 – PFB conversion (-) vs. time (h) for PS1-SH in case of eq. reaction for disulfide formation (full line) and in case of no eq. reaction for disulfide formation (dashed line) (thiol:DBU = 1:1, [thiol]₀ = 0.075 mol L⁻¹).

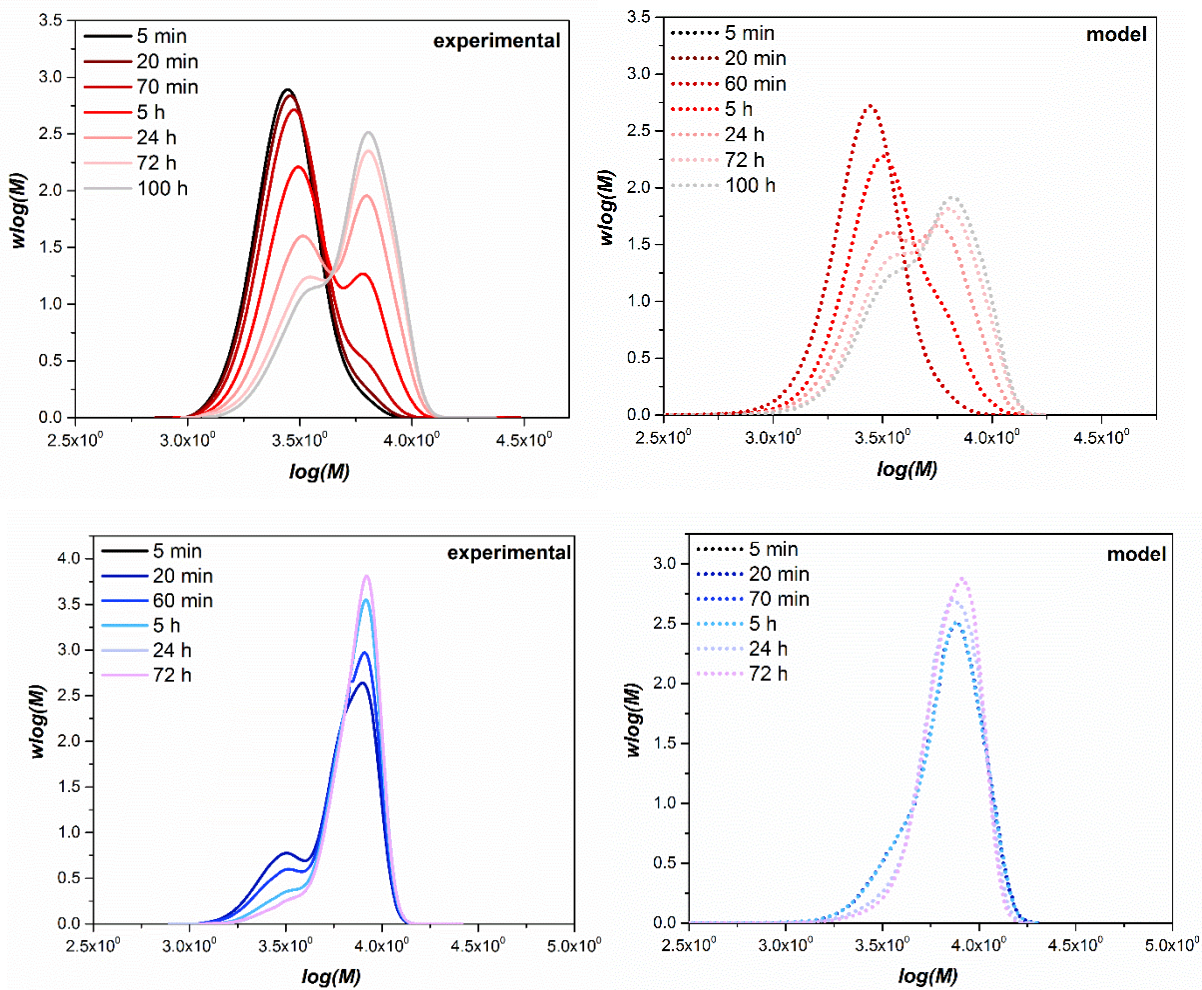


Figure S22 - SEC traces showing the evolution of PFTR employing 3PFB and PS2 in THF (red, top) and DMF (blue, bottom); $[\text{thiol}]_0 = 0.075 \text{ molL}^{-1}$, SH:base = 1:1; (left) experimental data and (right) simulated data.

Optimized condition for PFTR with a designed amount of TCEP

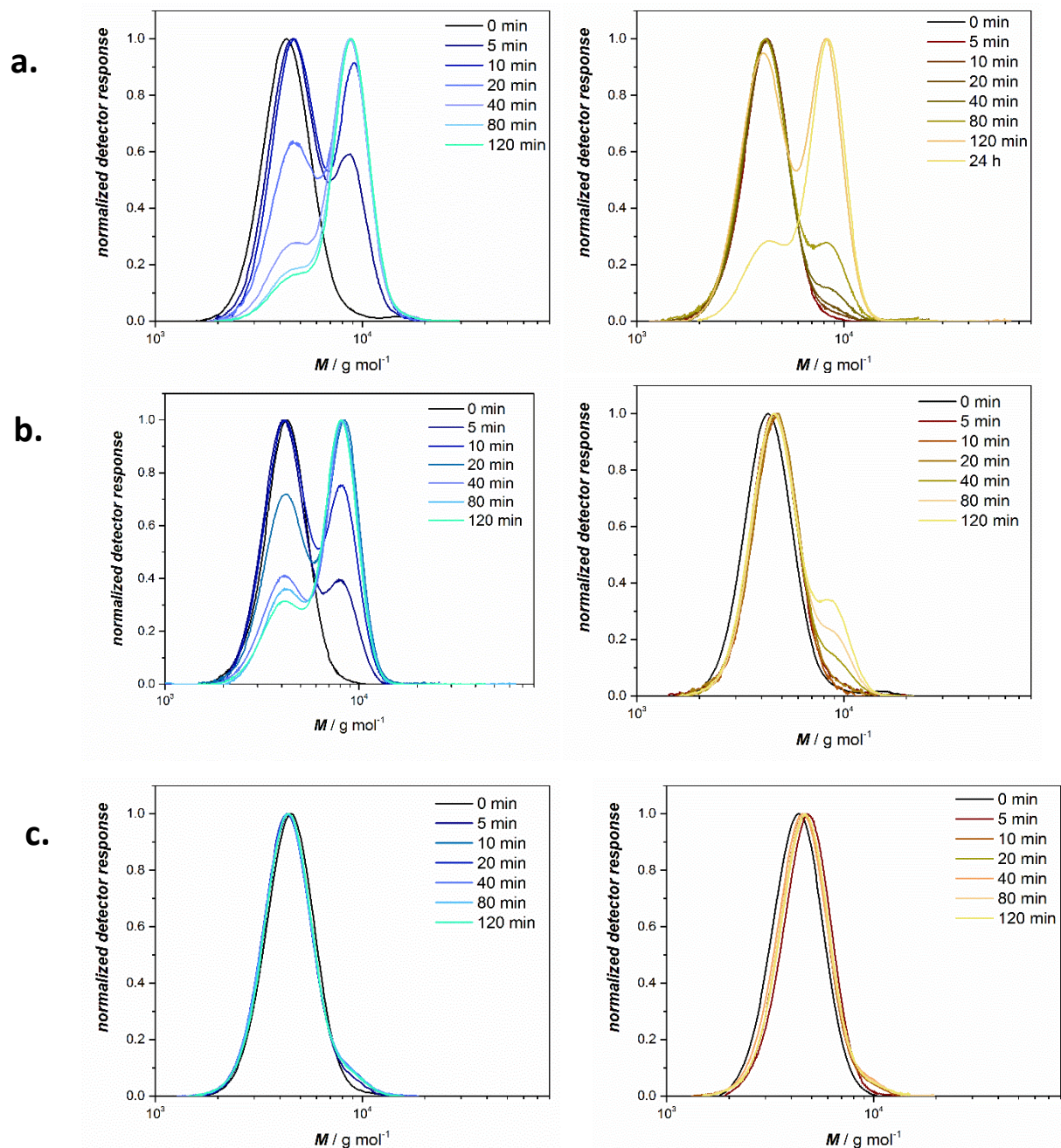
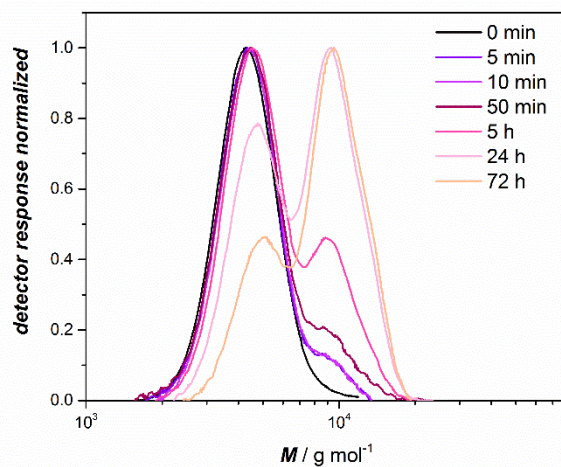
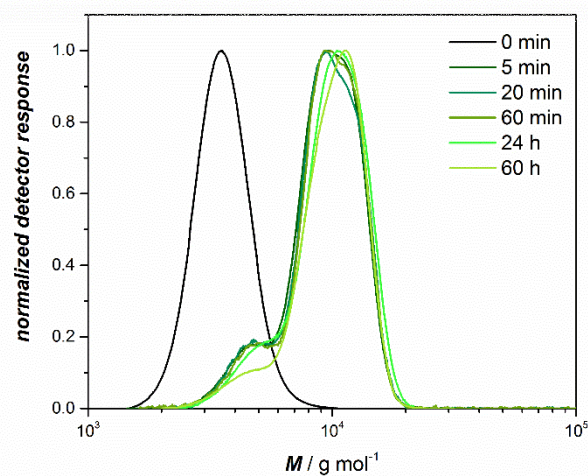


Figure S23 - SEC traces for the kinetic investigation on the disulfide bond formation reaction a. DMF (blue)/THF(yellow) in presence oxygen, b. DMF (blue)/THF(yellow) in absence of oxygen c. DMF (blue)/THF(yellow) in presence of TCEP and oxygen; $[\text{thiol}]_0 = 0.037 \text{ molL}^{-1}$, SH:base = 1:15.

a.



b.



c.

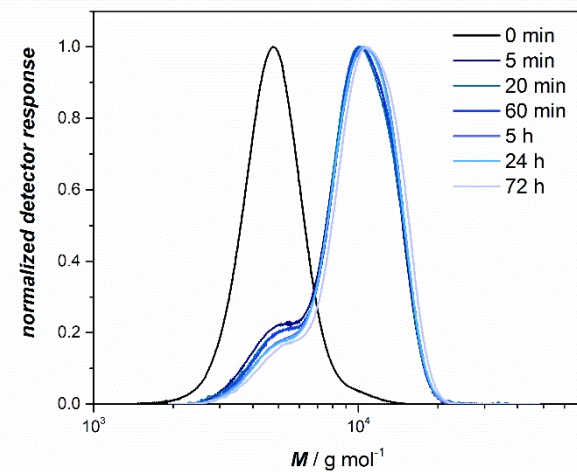


Figure S24 - SEC traces showing the evolution of PFTR employing 3PFB and PS1-SH, where PFB:SH groups have an initial ratio of 1:1 with **a.** the addition of 6 eq. of reducing agent, **b.** 1 equivalent of reducing agent or **c.** without reducing agent; $[\text{thiol}]_0 = 0.037 \text{ mol L}^{-1}$, SH:base:PFB group = 1:15:1.